www.czasopisma.pan.pl PAN POLSKA AKADEMIA NAUK www.journals.pan.pl

Arch. Metall. Mater. **63** (2018), 3, 1509-1512

DOI: 10.24425/123840

JUNG HYO PARK*#, SEONG LEE*, DONGHOON KIM*, YOUNGMOO KIM*, SUNG HO YANG*, SUNG HO LEE*

FABRICATION OF Mo-Si-B INTERMETALLIC COMPOUND POWDERS UNDER DIFFERENT HEAT TREATMENT CONDITIONS

In this research, we investigated the effects of reduction atmospheres on the creation of the Mo-Si-B intermetallic compounds (IMC) during the heat treatments. For outstanding anti-oxidation and elevated mechanical strength at the ultrahigh temperature, we fabricated the uniformly dispersed IMC powders such as Mo_5SiB_2 (T2) and Mo_3Si (A15) phases using the two steps of chemical reactions. Especially, in the second procedure, we studied the influence of the atmospheres (e.g. vacuum, argon, and hydrogen) on the synthesis of IMCs during the reduction. Furthermore, the newly produced IMCs were observed by SEM, XRD, and EDS to identify the phase of the compounds. We also calculated an amount of IMCs in the reduced powders depending on the atmosphere using the Reitveld refinement method. Consequently, it is found that hydrogen atmosphere was suitable for fabrication of IMC without other IMC phases.

Keywords: Mo-Si-B alloys, Intermetallic compounds, Reitveld refinement, T2 and A15 phase

1. Introduction

Mo-based silicide alloys have been investigated as one of the advanced ultra-high temperature structural materials to increase the temperature capability of hot section components in turbine engines [1]. It is attributed to the beneficial oxidation and creep resistance of the silicide compounds (e.g. Mo_5SiB_2 and Mo_3Si) and the excellent elevated mechanical and creep strengths of the α-Mo phases [2-3].

The alloys have been generally fabricated by ingot metallurgy; however, most melted Mo-Si-B alloys exhibit brittleness at ambient temperature due to the inherent heterogeneous microstructures [4]. Thus, researchers, including our group, have modified the microstructures of the alloys to enhance their fracture toughness with retaining the elevated mechanical strength by a powder metallurgical processing route. In those attempts, Byun et al. [5-8] introduced Mo-Si-B alloys obtained from core-shell intermetallic powders embedded by α-Mo particles. Since the alloys showed homogeneous distributed silicides within the continuous α- Mo matrix, their mechanical properties, especially fracture toughness, was slightly higher than those of melted Mo-Si-B alloys. However, in spite of the enhanced properties, the alloys still show a porosity of about 4% by presssureless sintering at 1400°C, which can be detrimental to the mechanical properties at elevated temperatures. Therefore, it is essential to investigate the overall consolidation processes of Mo-Si-B alloys, especially the fabrication of the alloyed powders to enhance the sinterability of the powders.

We demonstrated the influence of heat treatment conditions on the characteristics of Mo-Si-B alloyed powders. We controlled the reduction temperatures and atmospheres of as-milled Mo-Si-B particles to understand chemical reactions during reduction and the properties of the reduced powders. The features of the Mo-Si-B alloy powders were analyzed by X-ray diffraction and Rietveld analysis, scanning electron microscopy.

2. Experimental

In this research, we prepared raw powder materials, MoO_3, Si_3N_4 and BN for IMC powders and their mean particle sizes were 100.0 μm, 2.50 μm, and 1.0 μm, respectively. The morphologies and phase identification of the powders are shown in Fig. 1. The starting powders were milled with the composition of Mo-6.75Si-2.44B (wt%) by a ball-milling machine. The milling was carried out from 60 to 240 min at the speed of 75 rpm with tungsten carbide (WC) balls in a stainless steel jar. We evaluated the characteristics of the as-milled powders by using scanning electron microscopy (SEM), X-ray diffraction (XRD), and particles size distribution (PSD). Then, the milled particles were reacted with the two steps of heat treatments. In the first step, the as-milled powders were heated up to 900°C under H_2 atmosphere for reducing MoO_3 powders. The reduced powders, in the subsequent procedure, were also heated up to 1450°C and then held in 2 h with varying the atmosphere (e.g. vacuum, argon, and hydrogen) for producing the IMC (e.g. Mo_5SiB_2 (T2) and Mo_3Si

* AGENCY FOR DEFENSE DEVELOPMENT, P. O. BOX 35, YUSEONG-GU, DAEJEON, 34186 REPUBLIC OF KOREA

Corresponding author: melpjh@hanmail.net

(A15) phases) powders. To analyze their characteristics, we conducted SEM, XRD, and EDS, and especially, the amount of T2 and A15 phases in the IMC powders was also measured by using the Reitveld refinement calculations based on the XRD analysis.

3. Results and discussion

In the Fig. 1, the SEM images show the raw powders of MoO_3, Si_3N_4, and hBN, which have average size 100 µm, 2.5 µm, and 1 µm, respectively (Fig. 1 a-c). Also, the X-ray diffractions of raw powders are well matched with reference XRD data. (JCPDS, #05-0508, #41-360, and #34-0421, respectively) We measured the variation of powder size depending on the ball milling time. We carried out the ball milling process for 1 h, 2 h, 3 h, and 4 h and the optimized ball milling time is 3 h. This is because, the average surface area and d(0.5) are minimum vales at 3 h ball milling process (Table 1). Also, the ball milled powder has fine size compared to raw powders, under 1 µm and the crystal structures of MoO_3, Si_3N_4, and hBN aren't changed after ball milling process for 3 h (Fig. 2). The whole powder reactions followed blow equations:

$$MoO_3 + H_2 \rightarrow MoO_2 + H_2O \quad \text{(eq. 1)}$$

$$MoO_2 + 2H_2 \rightarrow Mo + 2H_2O \quad \text{(eq. 2)}$$

$$3Mo + 1/3Si_3N_4 \rightarrow Mo_3Si + 2/3N_2 \quad \text{(eq. 3)}$$

$$5Mo + 1/3Si_3N_4 + 2BN \rightarrow Mo_5SiB_2 + 5/3N_2 \quad \text{(eq. 4)}$$

TABLE 1

Particle size distribution analysis of as-milled powder condition for 1 h to 4 h

	Surface average (μm^2)	Volume average (μm^3)	d(0.1) (µm)	d(0.5) (µm)	d(0.9) (µm)	d(1) (µm)
1 h	0.329	10.424	0.156	0.314	45.439	96.63
2 h	0.288	4.574	0.157	0.263	11.765	96.13
3 h	0.279	4.349	0.154	0.251	11.809	95.94
4 h	0.463	10.347	0.211	0.485	38.339	151.11

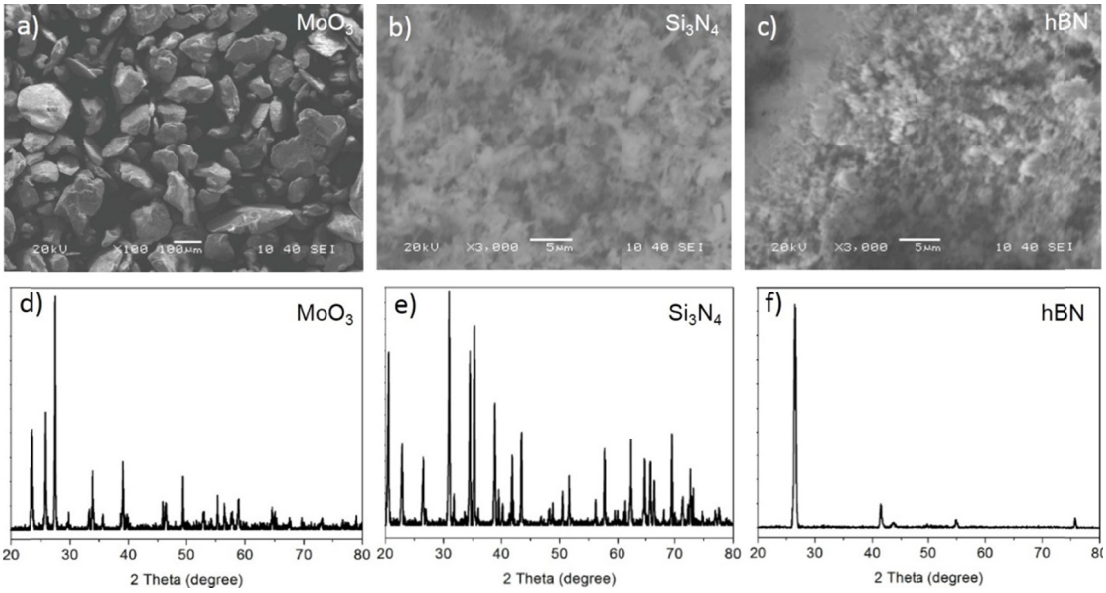

Fig. 1. SEM images and XRD peaks of raw power of a) and d) MoO_3, b) and e) Si_3N_4, and c) and f) hBN, respectively

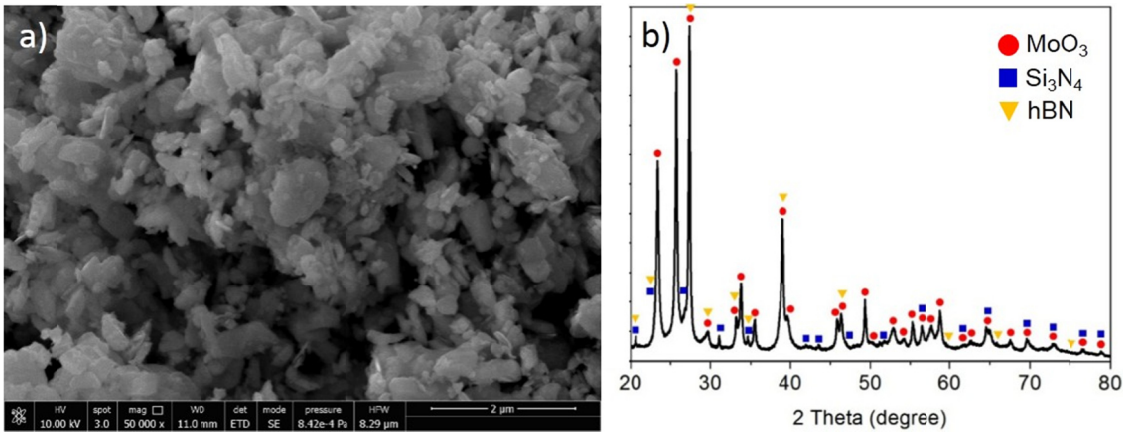

Fig. 2. a) Ball-milled powder for 3 h of a) SEM image and b) XRD peaks

In the first thermal treatment process, we carried out the reduction of MoO_3 at the 830°C and 900°C in the continuous furnace. The 1st reduced powders were observed by SEM and XRD (Fig. 3). The MoO_2 oxide powder remained in the 1st reduced powder from SEM image and XRD peaks (Fig. 3a and b). The remained MoO_2 give negative effect to generate T2 and A15 phases in the 2nd reaction step so we increased the reduction temperature to covert MoO_2 to pure Mo. The Fig. 3c and d show that all of the MoO_3 covert to the pure Mo after 900°C reduction process under hydrogen atmosphere. In the 2nd reaction process, we changed the atmosphere conditions such as vacuum, argon, and hydrogen because the IMC fabrication process used powder reaction is sensitive reaction comparing to the arc-melting method. In Fig. 4, we observed the surface and morphology of IMC powders which are treated in different conditions. All of the IMC have a same size and morphology, however the fabricated phases and peak intensity are different depending on the atmosphere (Fig. 4d-f). In the vacuum reaction, the Mo_2B is created but it isn't fabricated in the argon and hydrogen. Furthermore, we calculated weight percent of T2 and A15 which are changed depending on the atmosphere conditions (Table 2). The IMCs were polished and measured in SEM and EDS for observing the IMC phase (Fig. 5). In the vacuum condition, we can distinguish the phase difference as contrast change however we can't exactly index the kinds of phases. Under this situation, we select the 6 points in the IMC and compare the peak intensity of EDS (Fig. 5a and d). The P1 points have more large intensity of Mo and Si so we can suggest that the bright areas are T2 phase the dark areas are A15 phase. These results are also applied to the argon and hydrogen conditions. The P3 and P4 have different contrast and EDS intensities are different (Fig. 5b and e). The P4 points have large intensities of Mo and Si comparing to the P4 points so the P4 points are T2 phase but the P3 points have no Si signals which mean that P3 points are pure Mo phase. In case of hydrogen treatment, we also can distinguish the contrast difference in the IMC powder and the EDS intensities of P5 and P6 are different. The P6 points have a large intensity of Si so P6 points are A15 and P5 points are T2 phases (Fig. 5d and f).

TABLE 2

The weight percent of IMC depending on the atmosphere by Reitveld refinement calculation, (wt%)

	Mo	**Mo_5SiB_2 (T2)**	**Mo_3Si (A15)**	**Mo_2B**
Vacuum	10.1	22.8	22.8	5
Ar	3	35.2	61.8	
H_2	0.2	49.9	49.9	

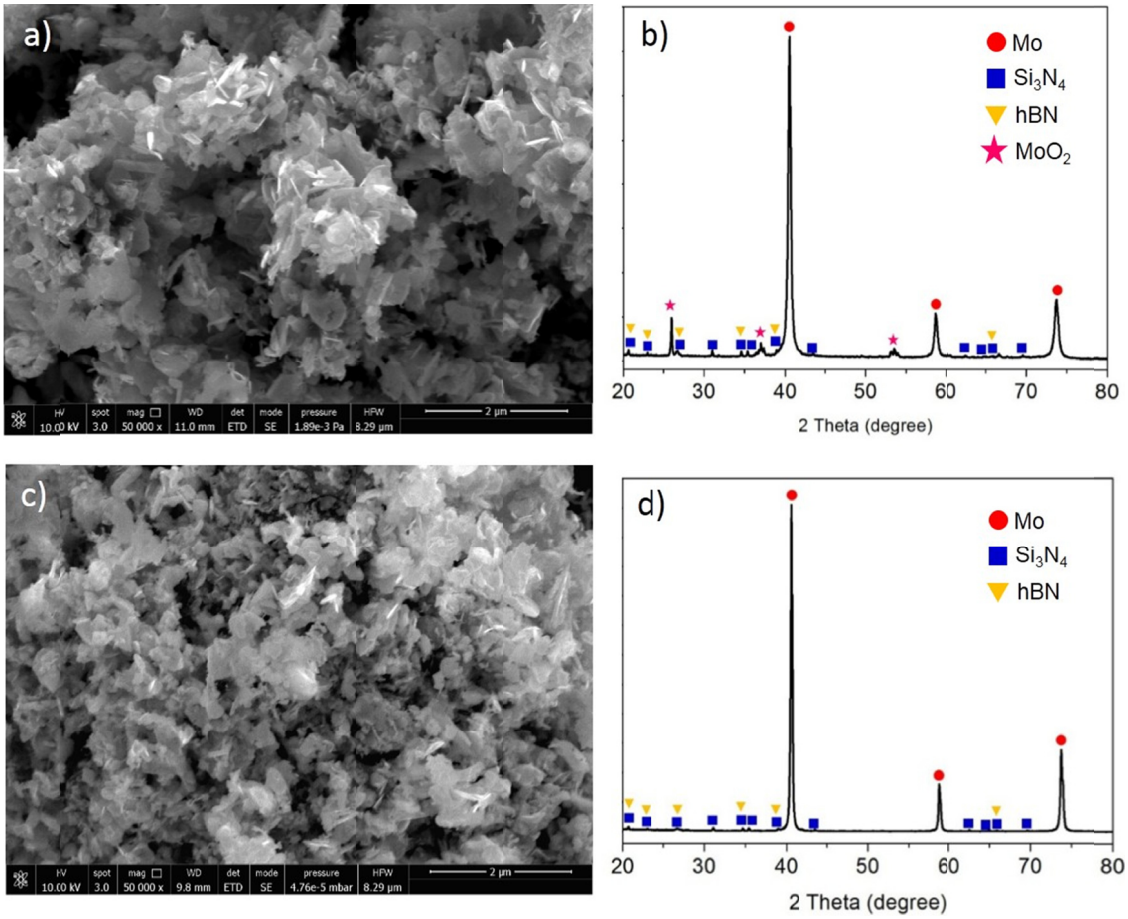

Fig. 3. a) SEM image and b) XRD peaks of the powder structure of 1st thermal reduction process at 830°C, c) SEM image and d) XRD peaks of the powder structure of 1st thermal reduction process at 900°C

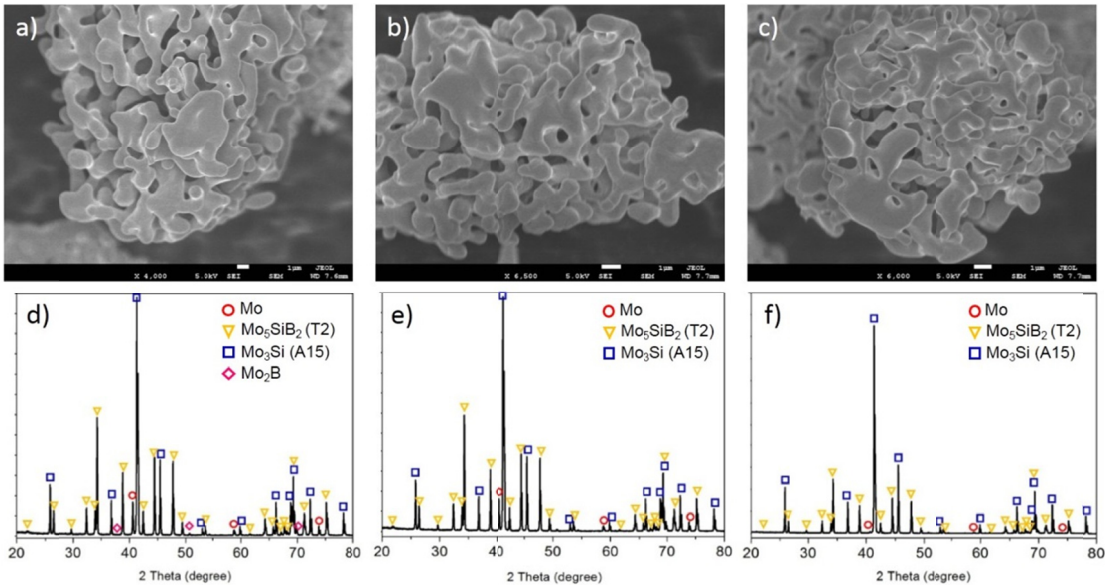

Fig. 4. The SEM images of IMC alloy in a) vacuum, b) argon, and c) hydrogen. The XRD peaks of IMC alloy in d) vacuum, e) argon, and f) hydrogen

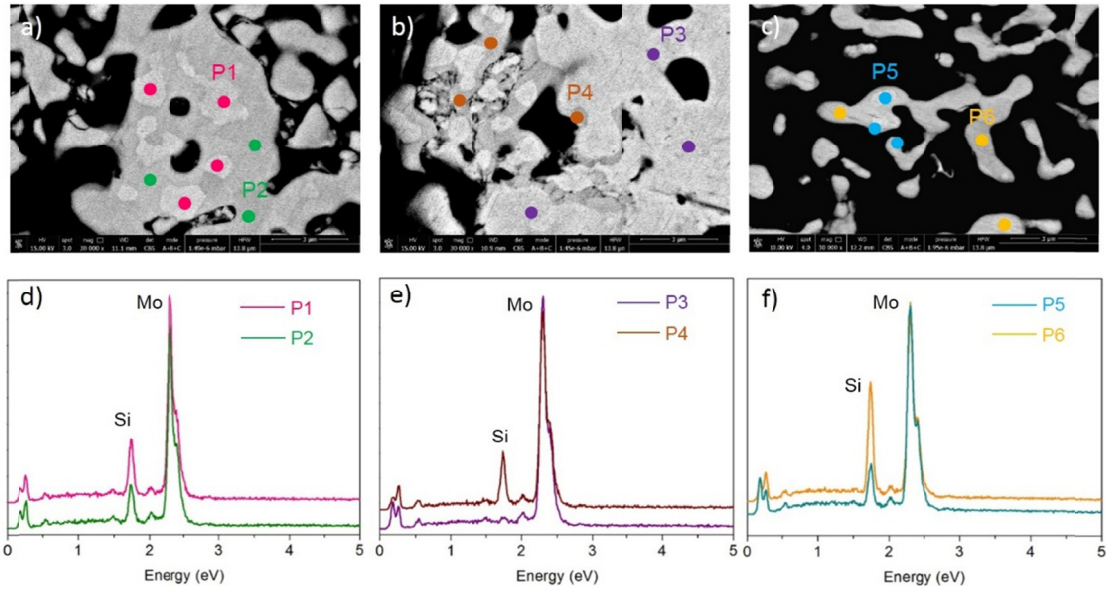

Fig. 5. The cross section SEM images in a) vacuum, b) argon, and c) hydrogen. The EDS peak intensity of d) vacuum, e) argon, and f) hydrogen

4. Conclusions

In this study, the IMC powders were fabricated using the MoO_3, Si_3N_4, and hBN powders to overcome the arc-melting method. The powder reactions were affected by atmosphere conditions. So we changed the reaction conditions such as vacuum, argon, and hydrogen to compare the morphology and weight percent of IMC calculated by Reitveld refinement. We found out that the weight percent of IMC was changed depending on the atmosphere and different IMC (Mo_2B) was fabricated in the vacuum condition. Also, we could observe the phase difference in the IMC from polished samples and the intensities of EDS peaks were changed depending on the phase difference.

REFERENCES

[1] D.M. Dimiduk, J.H. Perepezko, MRS Bulletin **28**, 639 (2003).
[2] K. Yoshimi, S-H. Ha, K. Maruyama, R. Tu, T. Goto, Adv. Mater. Res. **278**, 527 (2011).
[3] S-H. Ha, K. Yoshimi, K. Maruyama, R. Tu, T. Goto, Mater. Sci. Eng. A, **552**, 179 (2012).
[4] J.A. Lemberg, R.O. Ritchie, Adv. Mater. **24**, 3445 (2012).
[5] J.M. Byun, S-R. Bang, S.H. Kim, W.J. Choi, Y.D. Kim, Int. J. Refrac. Met. Hard Mater. **65**, 14 (2017).
[6] J.M. Byun, S-R. Bang, W.J. Choi, M.S. Kim, G.W. Noh, Y.D. Kim, Met. Mater. Int. **23**, 170 (2017).
[7] J.M. Byun, S.H. Hwang, S. Lee, M-J. Suk, S-T Oh, Y.D. Kim, Int. J. Refrac. Met. Hard Mater. **53**, 61 (2015).
[8] J.M. Byun, S-R. Bang, C.W. Park, M-J. Suk, Y.D. Kim, Met. Mater. Int. **22**, 81 (2016).